Proceedings of the ASME 2010 3rd Joint US-European Fluids Engineering Summer Meeting and 8th International Conference on Nanochannels, Microchannels, and Minichannels
FEDSM-ICNMM2010
August 1-5, 2010, Montreal, Canada

FEDSM-ICNMM2010-30290

EFFECT OF FINS ON VORTEX SHEDDING NOISE GENERATED FROM A CIRCULAR CYLINDER IN CROSS FLOW

Hiromitsu HAMAKAWA
Department of Mechanical Engineering
Oita University
Oita, 870-1192, JAPAN

Yuji KOUNO
Graduate School of Engineering
Oita University
Oita, 870-1192, JAPAN

Eiichi NISHIDA
Department of Mechanical Systems Engineering, Shonan Institute of Technology
Fujisawa, 251-8511, JAPAN

ABSTRACT

In the present paper, the effect of twist-serrated fins around a bare tube on the Aeolian tone was experimentally investigated. These fins were mounted spirally around a bare tube and had the same geometry as those actually used in boiler tubes. We measured the intensity of velocity fluctuation, spectrum of velocity fluctuation, coherence of Karman vortex in the spanwise direction, dynamic lift force, and sound pressure level of the aerodynamic noise generated from finned tubes with various fin pitches. An Aeolian tone induced by Karman vortex shedding was observed in the case of a finned tube, although the complicated fin was mounted around a bare tube. A decrease in the pitch of the fin effectively caused an increase in the equivalent diameter, which acted as the characteristic length of a cylinder with fins. The equivalent diameter depended on the Reynolds number. We modified a relation to calculate the characteristic diameter of the finned tube, which in turn was used to calculate the Strouhal number. The coherent scales in the spanwise direction for the cases with various fin pitches were slightly larger than that of a simple circular cylinder. It is known that the sound pressure level of the Aeolian tone depends on the coherent scale of the Karman vortex in the spanwise direction. However, when the pitch of the fins decreased, the peak level of the sound pressure spectrum decreased. A correlation analysis between the flow field and Aeolian tone was carried out.

INTRODUCTION

In heat exchangers such as commercially used boilers, acoustic resonant noise is occasionally generated in ducts when gas flows laterally with respect to the axis of the tubes. Details on the flow-induced vibration and noise in a heat exchanger can be found in some review papers [1-4].

The acoustic resonant noise generated by a heat exchanger is usually caused by the resonance of the acoustic modes inside the boiler and vortex shedding from the tube banks. Many studies have been published on the excitation mechanisms that cause acoustic resonance in the tube banks in cross flow [5-8]. Vortex excitation has been clearly shown to result from the formation of periodic vortices in the space between the tubes[7, 8].

Aeolian tones are the sounds produced by vortex shedding from a circular cylinder. These tones can induce vibrations in structures exposed to the sound pressure. If the frequency of the vortex shedding from the tubes in a heat exchanger coincides with the natural frequency of the heat exchanger cavity, the sound caused by the acoustic resonance can become so intense that it damages the heat exchanger. The far-field sound power of the Aeolian tone depends on the spanwise correlation length of the vortex shedding from a circular cylinder [9]. Therefore, if the correlation length of vortex shedding is less than that of a circular cylinder, the excitation energy of the acoustic resonance will be less than that in the case of a circular cylinder.

Recently, finned tubes have been used more frequently in heat exchangers to enhance heat transfer. These fins are mounted spirally around a bare tube surface because of easy production. It is generally believed that vortex-induced vibration can be suppressed by mounting helical strakes around a bare tube [9, 10]. Zdravkovich [10] showed that helical strakes or several fins as surface protrusions around a bare tube reduce vibration. However, loud resonant noise is occasionally generated in the duct when gas flows laterally to the axis of the finned tube banks. Some studies have reported the characteristics of the acoustic resonance and vortex shedding generated from finned tube banks. Nemoto et al. [11-13] suggested that acoustic resonance was generated even in finned tube banks. Chen [6], Kouba [14], Hamakawa et al. [15, 16], Kawaguchi et al. [17], and Ziada et al. [18] observed remarkable vortex shedding in finned tube banks or in the wake of a single finned tube.

On the other hand, it is known that a Karman vortex has a three-dimensional correlation structure in the span direction even in a two-dimensional flow field. Therefore, it is believed that the vortex is cut easily by the fins and that the vortex structure in the wake of a finned tube is different from that of a bare tube. Hamakawa et al. [16, 19] found that the spanwise scale of the vortex was considerably larger than the pitch of the fins. Ziada et al. [18] showed that the correlation length in the wake of a serrated finned tube changed with the angular rotation of the tube around its axis. This phenomenon seemed to be related to the irregular wavy pattern of the serrated fin distribution along the tube axis. The spanwise correlation length of vortex shedding is the basic parameter needed to estimate the characteristics of unsteady fluid forces and sound generation by vortex shedding from a finned tube. However, there have been very few studies on the characteristics of vortex shedding from a finned tube, and the characteristics of the Aeolian tone radiated from a finned tube are unclear.

A similarity law concerning the vortex shedding frequency from a circular cylinder is represented by the Strouhal number. There are two diameters in the case of a finned tube ‐ the fin diameter and the tube diameter ‐ that represent the characteristic lengths of the Strouhal number for a finned tube. Both diameters, however, are unsuitable for use as the characteristic length, because the vortex shedding frequency decreases with an decrease in the fin pitch. The fins effectively increase the tube equivalent diameter for the vortex shedding frequency. Thus, we proposed the equivalent diameter of the finned tube [15]. Furthermore, Mair et al. [20], Suzuki et al. [21], and Ziada et al. [18] reported that the vortex shedding frequency was correlated with the tube effective diameter. The equivalent diameter [15] is almost the same as the effective diameter proposed by Mair et al. [20] for small fin pitches, although the projected area for the gradient of the spiral parts of the fins are not included in the equivalent diameter. However, there have been few studies on the characteristic length of a finned tube, and the characteristics of the equivalent diameter are unclear.

The purpose of the present study is to clarify the effect of twist-serrated fins around a bare tube on the Aeolian tone and vortex shedding. Four tubes with similar shapes but different fin pitches are tested in a low-noise wind tunnel at Reynolds numbers in the subcritical regime. The characteristics of the equivalent diameter and the correlation between the Aeolian tone and the flow field around a finned tube for several fin pitches are discussed.

EXPERIMENTAL APPARATUS AND PROCEDURES

LOW-NOISE WIND TUNNEL

Our experiments were performed in a low-noise wind tunnel, which has been described in detail elsewhere [22]. This wind tunnel was an open-circuit with wing-type silencers in the diffuser located at the outlet of the blower and splitter-type silencers at the inlet of the blower. The test section was placed in the anechoic room, which was rectangular in shape, and 3 m long, 3 m wide, and 3 m high. The collector was downstream of the test section. Noise-absorbing furry materials were attached to the surface of the collector to reduce the interaction noise between the open jet and the collector. This collector was connected to a 3-m-long sound absorbent duct. The background noise was about 63 dB(A) at a freestream velocity of 50.0 m/s.

Figure 1 shows a schematic view of the test-section and a test cylinder. The cross section of the nozzle exit was a 0.3-m-wide and 0.3-m-high square. A finned tube was installed in the test section 100 mm downstream of the nozzle exit. The freestream velocity ranged from 2.5 m/s to 50.0 m/s at the test section inlet. The Reynolds numbers, based on tube diameter D and freestream velocity U_∞, ranged from 5.3×10^3 to 1.1×10^5. The flow past the nozzle was uniform, and the drift of the freestream velocity was less than about 0.9 %. The freestream turbulence level was less than 0.5 % of the freestream velocity. In addition, no peak of velocity fluctuation spectrum at the test section without the test cylinder was formed at this velocity range.

ACOUSTICAL CHARACTERISTICS OF END PLATES

Two end plates were placed at the top and bottom of the test section, and a test cylinder was placed vertically and rigidly supported between them. These were 900-mm-wide and 755-

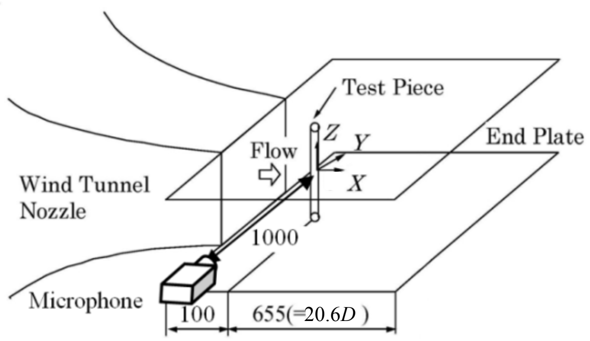

Fig.1 Schematic of test section and co-ordinate axes

mm-long acoustically non-reflecting end plates, which were large enough to cover the jet edge region. The downstream distance from the test cylinder to the edges of the end plates was 655 mm. These end plates were composed of a 25-mm-thick polystyrene porous material and 25-mm-thick glass wool backed with a punched steel plate to reinforce the plate rigidity [23].

Figure 2 shows the typical acoustic characteristics of these end plates. We measured the attenuation characteristics of the 1/3 octave-band levels of the wide-band noise radiated from a loudspeaker, which was placed between the end plates at one edge. It was clearly observed that the results for the non-reflecting end plates were almost the same as the attenuation characteristics of the free field. In this coordinate system, X was the flow direction, Z was the spanwise direction of the test cylinder, and Y was the transverse direction normal to both the X- and Y-axes, as shown in Fig. 1.

SHAPE OF FINNED TUBE AND CHARACTERISTICS LENGTH

Figure 3 show photographs of the finned tube. The fins were mounted spirally around a bare tube surface and were made from a 1.2-mm-thick plate with a height (width) of 12.7 mm by cutting 2-mm-wide and 7-mm-deep gaps. The edges of each needle-like fin were twisted at a small angle of about 25 degree. The fin shape of this twist-serrated fin was different from the fin in the paper by Ziada et al. [18]. Bare tube diameter D was 31.8 mm, fin diameter D_f was 57.2 mm, and the values used for fin pitch s were 25.4, 8.47, 5.08, and 3.63 mm, i.e., the ratios of the fin pitch per tube diameter, s/D, were 0.80, 0.27, 0.16, and 0.11, which are presented in Table 1. The span of the tube was 300 mm. These finned tubes had the same geometry as those actually used in boiler tubes.

The characteristic length of the Strouhal number of the finned tube was used for the equivalent diameter of the finned tube, D_e [16]. This diameter and Reynolds number R_e are defined by

$$\left.\begin{aligned} D_e &= D + \frac{(D_f - D)t_{\max}}{s} \\ R_e &= \frac{U_\infty D_e}{\nu} \end{aligned}\right\} \quad (1)$$

where D is the tube diameter, D_f is the fin diameter, s is the fin pitch, t_{max} is the maximum fin thickness perpendicular to the

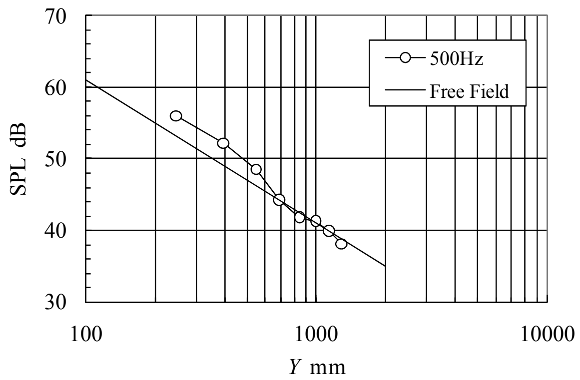

(a) 500 Hz

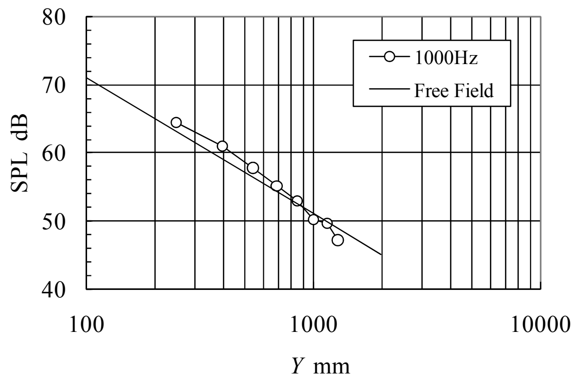

(b) 1000 Hz

Fig. 2 Acoustical characteristics of end plates

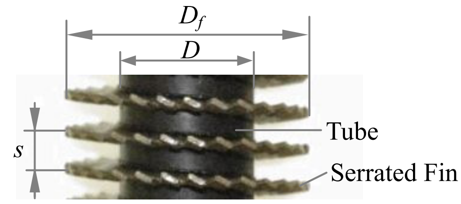

(a) Shape of twist-serrated fin

s/D=0.80 s/D=0.27 s/D=0.16 s/D=0.11

(b) Shape of twist-serrated finned tube

Fig. 3 Change in geometry of serrated fin

Table 1 Specifications of finned tubes

Fin type	s/D	s mm	D mm	D_f mm	t mm	n
Serrated fin	0.80	25.4	31.8	59.2	1.2	1
Serrated fin	0.27	8.47	31.8	57.2	1.2	1
Serrated fin	0.16	5.08	31.8	57.2	1.2	1
Serrated fin	0.11	3.63	31.8	57.2	1.2	1
Bare tube 1	-	-	31.8	-	-	-
Bare tube 2	-	-	57.2	-	-	-

spiral axis, U_∞ is the freestream velocity, and ν is the kinematic viscosity.

MEASUREMENT OF AERODYNAMIC NOISE

The aerodynamic sound in the far field from the test tube was measured at X=0 mm, Y=1000 mm, and Z=0 mm using a microphone. When the observation location was far enough to be considered as the far field, the effect of the near field could be neglected. In this measuring position, the near field component attenuates, and the far field component is about 10 dB larger than the near field component for phenomena that occur over 170 Hz. The microphone output was sampled by an FFT analyzer and the statistical parameters were calculated. The spectra of the sound pressure level (SPL) were calculated for 80 ensemble averages of 2048 data points that were sampled at 2.56 kHz. The frequency resolution was estimated to be 1.25 Hz.

MEASUREMENT OF FLOW FIELD IN THE WAKE

Figure 4 shows a schematic of the flow field test. A hot-wire anemometer was used to measure the flow in the wake of the test tube. The mean velocity and velocity fluctuation in the wake of the tube were measured using an I-type hot-wire sensor, using tungsten wires with a diameter of 5 μm and a sensor length of 1.25 mm. The hot-wire sensor was placed parallel to the span (Z-axis) direction to measure the velocity fluctuation due to vortex shedding from the tube. The hot-wire sensor was traversed and fixed at a pre-determined location in the wake of the tube. The characteristics of flow, such as the velocity distribution of the mean flow and turbulence intensity, and the spectrum of velocity fluctuation were measured on the X-Y plane at different positions in the wake of the tube. The coefficient of velocity fluctuation was defined as the ratio of the intensity, u' (i.e., the standard deviation of velocity fluctuation), to the main flow velocity, U_∞, i.e., u'/U_∞.

Another hot-wire probe was installed when the coherence and phase between the velocity fluctuations at two different locations were measured. The outputs from these hot-wire anemometers were automatically sampled by an FFT analyzer and a PC-based acquisition system, and then the statistical parameters were calculated. The anemometer data was linearized before any spectral calculations were performed. The hot-wire signals were digitized using a sampling frequency of 2.56 kHz. The Fourier power spectra of the signals were based on an average of 80 runs, where each run included 1024 or 2048 samples. The frequency resolutions were estimated to be 2.5 or 1.25 Hz, respectively. The analysis of the data was accomplished using an FFT analyzer to calculate the coherence and phase for the turbulence and sound data.

MEASUREMENT OF FLUCTUATING LIFT FORCES

Figure 5 shows a schematic of the load test. Measurements of the fluctuating lift forces on the test tube were performed using a load cell and amplifier. One side of the load cell was supported at the edge of the test tube, while the other side was fixed at the mass bed. The other side of the test tube was a free edge, and it vibrated at infinitesimal amplitude at a freestream of about 50 m/s. Measurements of the aerodynamic sound in the far field were performed prior to the load test. The test results for aerodynamic sound were in good agreement with those for no vibration. Thus, the effect of an infinitesimal vibration on aerodynamic sound could be neglected. Data was logged using a PC-based acquisition system, which had a sampling frequency of 4 kHz for the load cell. The frequency resolutions were estimated to be 1.95 Hz. The natural frequency of the test tube, load cell, and mass bed system was about 80 Hz. The fluctuating lift force signals were extracted analytically from the outputs of the load cell using a band-pass filter generated by MATLAB-based software; these signals included the noises of natural frequency and its overtones. The frequency of the fluctuating lift forces was identified from the vortex shedding frequency measured using a hot-wire and microphone.

EXPERIMENTAL UNCERTAINTIES

The resolutions of the FFT results at about freestream velocity of 50.0 m/s were 1.25–2.5 Hz, so the uncertainty estimates caused by the resolution of S_t was less than ± 1.5 % for all cases. The sampling frequencies for each spectrum measurement at different freestream velocity were adjusted to be suitable sampling interval. The uncertainty estimates was based on 95 % confidence levels. The overall uncertainties in SPL, f_p, u'/U_∞, S_t, R_e, and C_L/C_{L0} were estimated to be ± 3 %,

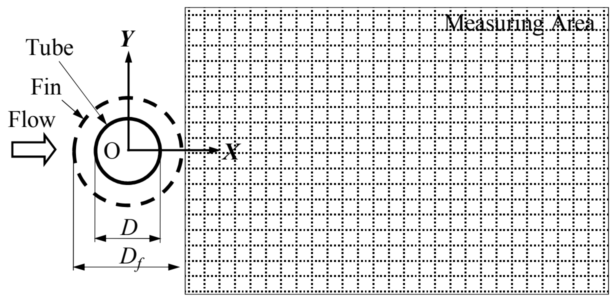

Fig. 4 Schematic of flow field test

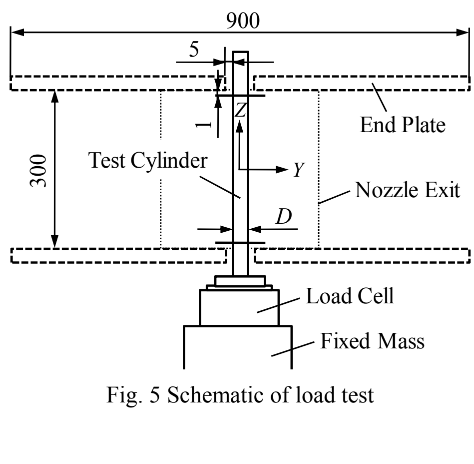

Fig. 5 Schematic of load test

±2 %, ±3.5 %, ±2.5 %, ±1.5 %, and ±3 %, respectively.

RESULTS AND DISCUSSION

AERODYNAMIC NOISE GENERATED FROM A FINNED TUBE

The spectra of the sound pressure level (SPL) of the aerodynamic sound radiated from the test tubes were measured. Figure 6 shows the spectra of the relative SPL, which were based on the peak SPL of 87.2 dB for bare tube 1 (BT1), together with the background noise, which was the wind tunnel noise without a test tube as shown in the gray heavy lines. In Fig. 6, BT1 represents the results for a bare tube of D=31.8 mm. A single high peak is formed at 310.0 Hz in the spectrum, which corresponds to the shedding of Karman vortices with a Strouhal number of 0.200. Similarly, bare tube 2 (BT2) represents the result for a bare tube, whose outer diameter was considered to be the fin diameter D_f=57.2 mm. The Strouhal number was about 0.204. However, the peak level is approximately 4.7 dB lower than the bare tube of D=31.8 mm. This is probably ascribable to end effects. Because the tube

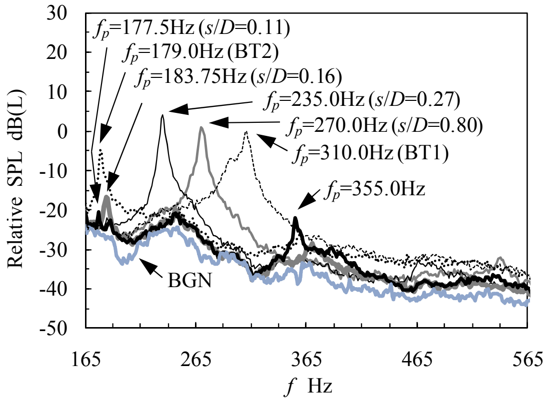

Fig. 6 Comparison of spectra of relative SPL (U_∞=50.0m/s, R_e=1.1×10^5-1.9×10^5)

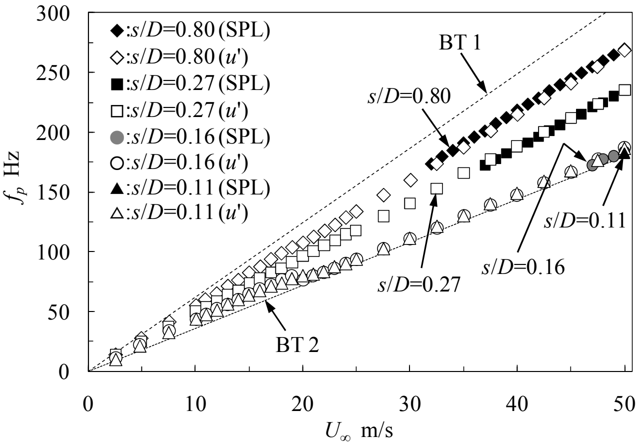

Fig. 7 Variation in peak frequency against freestream velocity

diameter of BT2 increased compared to the case of BT1, the aspect ratio between the height of the test section and the tube diameter became small. This means a shorter cylinder at the case of BT2 compared with that of BT1. The blockage of the bare tube for D=31.8 mm was 10.6 % of the cross-sectional area at the nozzle exit, while that of D_f=57.2 mm was 19.1 %.

The peak SPL of the spectrum varied with the fin pitch. In Fig. 6, the gray fine line shows the results for a finned tube of s/D=0.80. A single high peak is formed at 270.0 Hz in the spectrum, which is the same as the level of the bare tube of D=31.8 mm, while the peak frequency is about 40.0 Hz lower than that of the bare tube. The solid line shows the results for s/D=0.27. The peak level for s/D=0.27 is approximately 3 dB higher than that for the bare tube of D=31.8 mm, while the peak frequency is 75.0 Hz lower than that for the bare tube. When the pitch of the fins decreased, the peak level and peak frequencies of the SPL spectrum decreased. The peak levels for s/D=0.16 and 0.11 are approximately 11.9 and 15.8 dB lower than that for the bare tube of D_f=57.2 mm, respectively. The peak frequencies are about 126.25 and 132.5 Hz lower than that of the bare tube of D=31.8 mm, and agree with the peak frequency for D_f=57.2 mm. On the other hand, the peak frequency of 355.0 Hz for s/D=0.11 is the harmonic of 177.5 Hz. As the pitch of the fins decreased, the peak level of harmonic components increased.

The effect of the near field can be neglected over 170 Hz for the aerodynamic sound of the far field. Variations in the peak frequency over 170 Hz are plotted against the freestream velocity, U_∞, in Fig. 7. The closed symbols and solid gray symbols represent the results of aerodynamic noise. As the pitch of the fins decreased, the peak frequencies decreased. However, the peak frequencies for s/D=0.16 and 0.11 are in good agreement with that for a bare tube of fin diameter D_f=57.2 mm.

VORTEX SHEDDING CHARACTERISTICS FOR A FINNED TUBE

We measured the velocity fluctuations in the wake of a finned tube to clarify the mechanism of change for the peak level of SPL for all fin pitches. The distributions of the turbulence intensity in the wake of the finned tubes are shown in Figs. 8(a)–(d) as contour maps of the coefficient of the velocity fluctuation, u'/U_∞. u' refers to the total r.m.s. amplitude of the velocity fluctuations. The locations of the contour map measurements were normalized with the equivalent diameter D_e or the tube diameter D. The double circle with a dotted line on the left side of the figure shows the location of a finned tube. There were two regions where the velocity fluctuation became intense on both sides just downstream of a finned tube, as shown in Figs. 8(a) – (d). The distributions of u'/U_∞ are asymmetrical with respect to the X-axis (Y=0) in detail. This was caused by the asymmetric shape of the finned tube. The overall distributions are almost symmetric with respect to the X-axis. As the pitch of the fins decreased, the maximum points of turbulence intensity

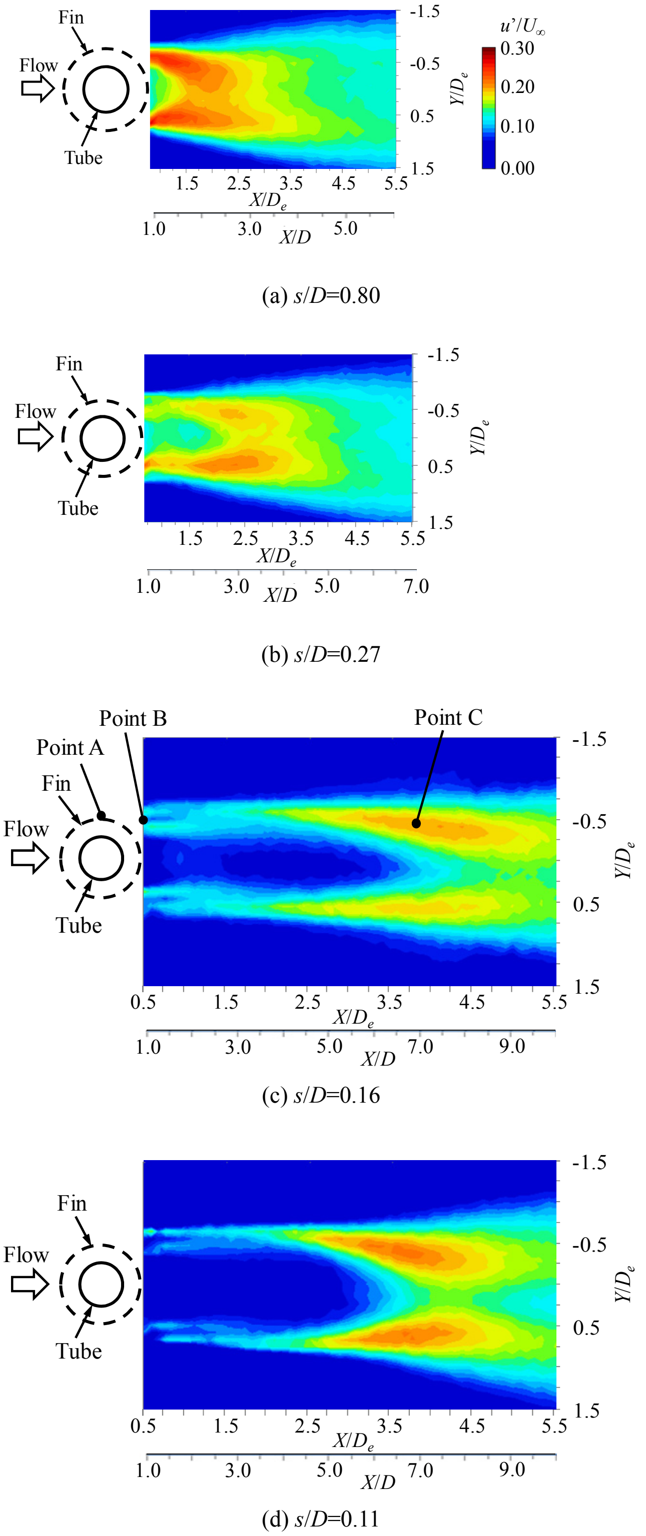

Fig. 8 Contour maps of coefficient of velocity fluctuation in the wake of a finned tube (U_∞=50.0 m/s, R_e=1.1×10^5-1.9×10^5)

were shifted to the downstream side, except for s/D=0.11. Moreover, a dead water region with weak turbulence intensity appeared widely behind the finned tubes of s/D=0.11 and 0.16. The contour map of the finned tube for s/D=0.16 is similar to that of s/D=0.11, with the exception of the maximum value of turbulence intensity and the spread of the dead water region exhibiting a smaller turbulence intensity behind the finned tube.

Figure 9 shows profiles of the turbulence intensity along the Y coordinate for all fin pitches in the near wake of the finned tube. As noted later, D_e was modified as the characteristic length for the finned tubes, and the location of the turbulence intensity measurement was normalized with this modified D_e. As the pitch of the fins decreased, the turbulence intensity in the near wake of the finned tube decreased. Four peaks were found at about Y/D_e=±0.4 and ±0.6 in the turbulence intensity profiles for s/D=0.11 and 0.16. These positions corresponded to the separated shear layers behind the finned tube, as shown Figs. 8(c) and (d). Thus, as the pitch of the fins decreased, the turbulence intensity of the separated shear layer in the near wake of the finned tube decreased.

The turbulence intensity of the outer separated shear layers at about Y/D_e=±0.6, X/D_e=0.8–1.9 for s/D=0.11 became intense compared to that of the inner shear layers at Y/D_e=±0.4, as shown in Figs. 8 and 9. The flow separated mainly from the outside of the fins mounted around a bare tube for s/D=0.11, because it was not easy to flow at the inside of the narrow gaps between the serrated fins. The peak frequency of the SPL spectrum for s/D=0.11 agreed well with that of a bare tube of D_f=57.2 mm, which was the same as the fin diameter. On the other hand, the intensity of the inner separated shear layers at about Y/D_e=±0.4, X/D_e=0.8–1.9 for s/D=0.16 was greater than that of the outer shear layers. This was due to the leakage flow from the gaps between the serrated fins with the increase in fin pitch. The spread of the separated shear layer was caused by the interaction between this flow and the free shear layer separated from the outside of the fins mounted around the bare tube. Thus, the maximum value of turbulence intensity and the

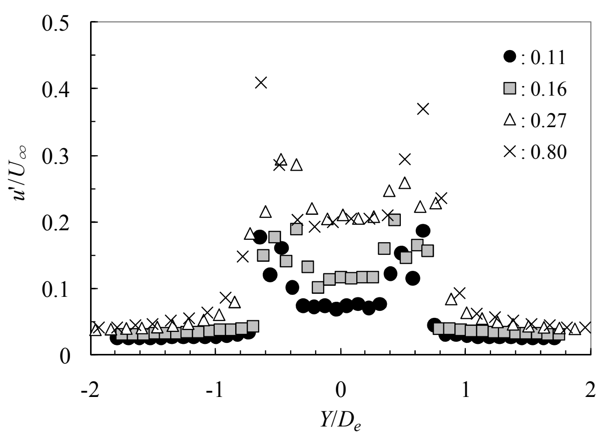

Fig. 9 Profiles of turbulence intensity in the near wake of a finned tube (X/D_e=0.84, U_∞=50.0 m/s, R_e=1.1×10^5-1.9×10^5)

distribution of the dead water region for s/D=0.11 changed slightly compared to those for s/D=0.16. The peak frequency of the SPL spectrum for s/D=0.16 agreed well with that of a bare tube of D_f=57.2 mm and s/D=0.11. It was observed that if the fin pitch became smaller, the leakage flow rate decreased and the characteristics of vortex shedding were close to those of a bare tube of D_f=57.2 mm.

Figure 10 shows profiles of the turbulence intensity along the Y coordinate for all fin pitches measured at the points of maximum turbulence intensity ($u'_{\max}$ point) in the streamwise direction. The turbulence intensities became most intense at X/D_e=1.3, 2.2, 3.8, and 3.6 for s/D=0.80, 0.27, 0.16, and 0.11, respectively, as seen in Fig. 8. Furthermore, the bare tubes for BT1 and BT2 were at X/D_e=1.2. The fins had the effect of decreasing the turbulence intensity. The turbulence profiles, except for s/D=0.11, show a gradual transition with decreased fin pitch from the bare tube to finned tubes of s/D=0.16. However, the maximum turbulence intensities are approximately the same for s/D=0.27, 0.16, and 0.11, between 0.30 and 0.32. Measurements at different Reynolds numbers and fin shapes showed similar features in Ziada et al. [19]. The profile of the finned tube for s/D=0.27 is similar to the profiles for s/D=0.16 and 0.11, with the exception of exhibiting a smaller turbulence intensity deficit at the wake center line. The maximum turbulence intensities for s/D=0.27, 0.16, and 0.11 are about 15-20% lower than those of bare tubes.

Figure 11 shows profiles of the streamwise turbulence intensity for all fin pitches measured at the $u'_{\max}$ point in the transverse direction. At X/D_e=1.0-1.5, as the pitch of the fins decreased, the turbulence intensities decreased. The velocity fluctuations at the near wake were caused by the fluctuation of the free shear layer separated from the surface of the finned tube. The turbulence intensities for s/D=0.16 and 0.11 were about 48 and 45% of the bare tube case, respectively. This indicates that the separation shear layers in the near wake for s/D=0.16 and 0.11 were stable compared with that of the bare tube.

As X/D_e increased, the turbulence intensities gradually became closer to the same value. At X/D_e=2.5–3.0, the turbulence intensities were approximately the same for all fin pitches, at about 0.25–0.30. This is similar features in Ziada et al. [19]. As X/D_e increased over about 3.0, the turbulence intensities for s/D = 0.16 and 0.11 increased until they reached the maximum levels, and those for s/D=0.8 and 0.27 and the bare tube decreased. Over X/D_e=2.0, the turbulence intensities were approximately the same for s/D=0.8 and 0.27 and the bare tubes.

Figure 12 shows the effect of the Reynolds number on the turbulence intensity profiles measured at the $u'_{\max}$ point in the transverse direction for s/D=0.16. As the Reynolds number increased, the maximum points of turbulence intensity were shifted to the downstream side, and their maximum values decreased slightly. However, at X/D_e=1.0, the turbulence intensities were approximately the same for $R_e=3.1\times10^4$–1.9×10^5, at about 0.20. It is clear that the turbulence intensity in the near wake of the finned tube at about X/D_e=1.0 did not depend on the Reynolds number between 3.1×10^4 and 1.9×10^5.

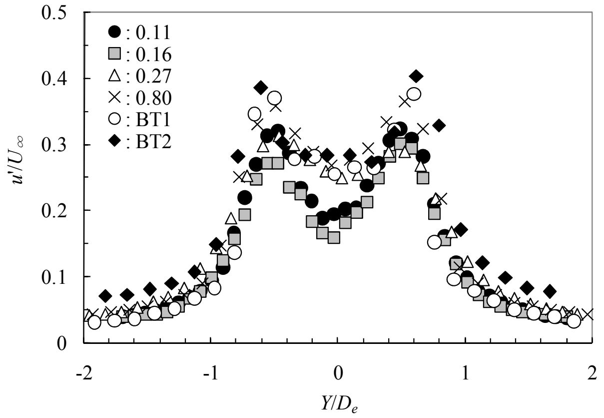

Fig. 10 Profiles of turbulence intensity at u'_{max} point in streamwise direction (s/D=0.80:X/D_e=1.3, s/D=0.27:x/D_e=2.2, s/D=0.16: X/D_e=3.8, s/D=0.11:X/D_e=3.6, BT1:X/D_e=1.2, BT2: X/D_e=1.2 , U_∞=50.0 m/s, $R_e=1.1\times10^5$-1.9×10^5)

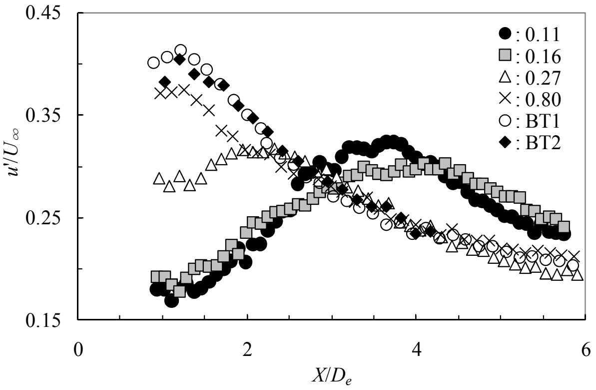

Fig. 11 Profiles of streamwise turbulence intensity at u'_{max} point in transverse direction (U_∞=50.0 m/s, $R_e=1.1\times10^5$-1.9×10^5)

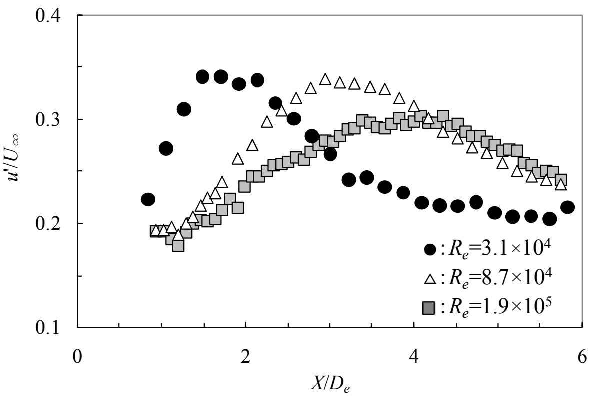

Fig. 12 Profiles of streamwise turbulence intensity in the wake of a finned tube (s/D=0.16)

Next, we measured the spectrum of velocity fluctuation in the wake of the finned tube. Figure 13 shows the typical spectra of velocity fluctuations at the $u'_{\max}$ point in Fig. 8. Figures 13(a) and (b) are the results for s/D=0.16 and 0.11 respectively. Evidently, in the case of s/D=0.16 and 0.11, single high peaks were formed at 185.0 Hz and 177.5Hz, which suggests the existence of a periodic phenomenon even though the peak levels of SPL decreased by about 11.9 and 15.8 dB from that for a bare tube of D_f=57.2 mm, as shown in Fig. 6. These peak frequencies are in good agreement with the SPL results in Fig. 6. The peak level of the spectrum for s/D=0.11 is larger than that for s/D=0.16, which is in good agreement with the feature of the turbulence intensity in Figs. 8, 10 and 11. It is clear that the periodicity of the velocity fluctuation in the wake of a finned tube for s/D=0.11 becomes intense compared with that for s/D=0.16, even though the peak level of SPL for s/D=0.16 is slightly larger than that for s/D=0.11. Similarly, single high peaks were formed in the spectra for other fin pitches in the present experiment, and these peak frequencies were in good agreement with the SPL results in Fig. 6. These features are described in the next session.

Next, we measured the phase delay of the velocity fluctuations by using the two-point measurements procedure. Hot-wires were installed at the intense velocity fluctuation points on both sides just downstream of the finned tube. Figure 14 shows the typical phase delay for s/D=0.16. The phase delay at the peak frequency of velocity fluctuation was about 180 degree. This means that the velocity fluctuations were out of phase with each other, which is a typical characteristic of Karman vortex shedding. Similar tendencies were obtained at other fin pitches and bare tubes in the present experiment. Thus, the periodic velocity fluctuations discussed above were caused by the Karman vortex shedding, although the maximum points of turbulence intensity moved to the downstream side at the small fin pitches. It is noteworthy that the vortex shedding phenomenon had a strong periodicity in the wake of the finned tube for small fin pitches, even though the velocity gradient became weak in the separation shear layer.

VORTEX SHEDDING FREQUENCY AND CHARACTERISTICS LENGTH

In Fig. 7, the open symbols or the symbols for u' show the changes in the peak frequencies of the velocity fluctuation measured at the u'_{max} point, which were plotted against the freestream velocity. The closed symbols and the solid gray symbols or the symbols for SPL are the results for the peak frequencies of SPL. The peak frequencies of the velocity fluctuations were in good agreement with the SPL results. The peak frequency of the spectrum increased in proportion to the freestream velocity for s/D=0.80 and 0.27 and for bare tubes. However, for s/D=0.16 and 0.11, the peak frequencies were close to that for a bare tube of D_f=57.2 mm over about U_∞=20.0 m/s.

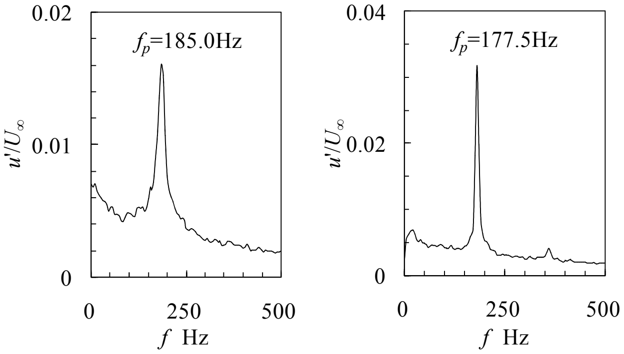

(a) s/D=0.16 (b) s/D=0.11

Fig. 13 Spectral distributions of u'_{max} point in the wake of a finned tube (R_e=1.9×10^5)

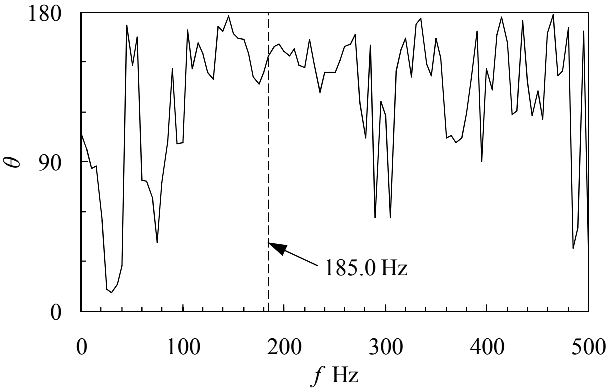

Fig. 14 Phase delay of velocity fluctuations by two-point measurements procedure (s/D=0.16, R_e=1.9×10^5)

Under U_∞=18.0 m/s, the peak frequency of the spectrum increased in proportion to the freestream velocity for all fin pitches. The peak frequencies decreased as the fin pitch decreased. That is, the frequencies of the vortex shedding from finned tubes were in between the vortex shedding frequencies for bare tubes of D=31.8 mm and D_f=57.2 mm. This indicates that a finned tube can be simply considered as a single bare tube for the vortex shedding. It can be understood that the equivalent diameter increases as the pitch of the fin becomes small because the fin changes the equivalent diameter of the finned tube.

On the other hand, the gradients of the peak frequencies for s/D=0.16 and 0.11 against the freestream velocity changed at a freestream velocity of about 19.0 m/s, and the peak frequencies of these fin pitches agreed well with that of a bare tube with a fin diameter over 20.0 m/s. This indicates that the flow separates from the outside of the fins and the equivalent diameter of the finned tube agrees with the fin diameter. The equivalent diameter of a finned tube depended on the Reynolds number and changed suddenly when the pitch of the fins was suitably small. Therefore, we modify the equation of equivalent diameter and add a condition for the application of the fin shape and Reynolds number as follows.

$$\left.\begin{array}{l} D_e = D_f \\ (s/D \le 0.16,\ 7.6\times10^4 \le R_e \le 1.9\times10^5) \end{array}\right\} \quad (2)$$

where D is the tube diameter, D_f is the fin diameter, s is the fin pitch, t_{max} is the maximum fin thickness perpendicular to the spiral axis, U_∞ is the freestream velocity, ν is the kinematic viscosity, R_e is the Reynolds number, and D_e is the equivalent diameter of the finned tube.

Figure 15 shows the Strouhal number, S_t, against the Reynolds number, R_e, obtained by using the modified equivalent diameter, D_e, defined in equation (2) as a characteristics length, along with the experimental data of the vortex shedding frequency, f_p. S_t is defined as follows:

$$S_t = \frac{f_p D_e}{U_\infty} \quad (3)$$

The Reynolds number ranged from 1.0×10^4 to 1.9×10^5 and was less than the critical Reynolds number. The values of S_t were within the range of 0.185 to 0.224. There was a scatter for S_t because the effect of the fins on the vortex shedding differed depending on the shape and pitch of the fins for the Reynolds number. It is clear that the equivalent diameter can be calculated from equation (1) and (2) in the Reynolds number range of 1.0×10^4 to 1.9×10^5, even though the shape of the body is quite different from a circular cylinder.

SPANWISE VORTEX STRUCTURE

It is known that the intensity of the Aeolian tone generated from a circular cylinder depends on the spanwise correlation length of the pressure fluctuation due to vortex shedding. Even in a two-dimensional flow field, the Karman vortex has a three-dimensional correlation structure in the span direction [9]. Hamakawa et al. [16, 19] found that the spanwise scale of the vortex was considerably larger than that of a bare tube. Ziada et al. [18] showed that the correlation length in the wake of a serrated finned tube changed with the angular rotation of the tube around its axis, and the coherent vortex scales in the spanwise direction of a finned tube were almost the same as that of a simple circular cylinder. However, in the present study, when the pitch of the fins decreased, the peak level of the SPL spectrum decreased, as shown in Fig. 6.

We measured the coherence of the velocity fluctuations at a freestream velocity of 50.0 m/s. One probe was set at the u'_{max} point (reference point, Z=0) and the other probe was traversed along the span direction through the u'_{max} point, as shown in Fig. 8. Figure 16 show the distribution of the coherence, C_{xy}, at the vortex shedding frequency along the span direction. The coherence is symmetrically distributed with respect to the point Z=0 in Fig. 16. The coherent distributions in the spanwise direction of finned tubes for all fin pitches were between 0.8 and 1.0, which were slightly larger than that of bare tube 2. This means that the spanwise vortex scale in the wake of the finned tube did not decrease compared with that of a bare tube. Thus, the sizes of the spanwise coherent scales of the Karman vortex were not the reason for the reduction in the peak SPLs of s/D=0.16 and 0.11. On the other hand, the values

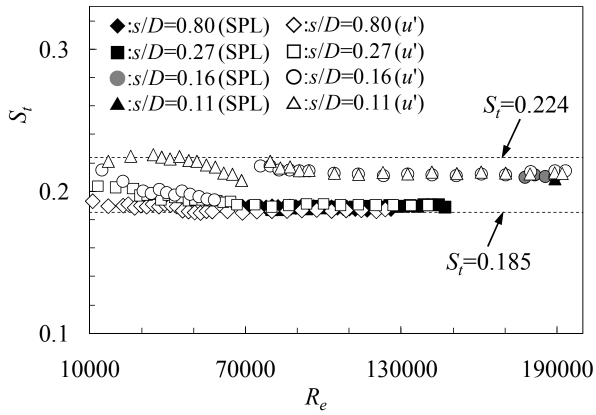

Fig. 15 Strouhal number defined based on equivalent diameter dependence on Reynolds number

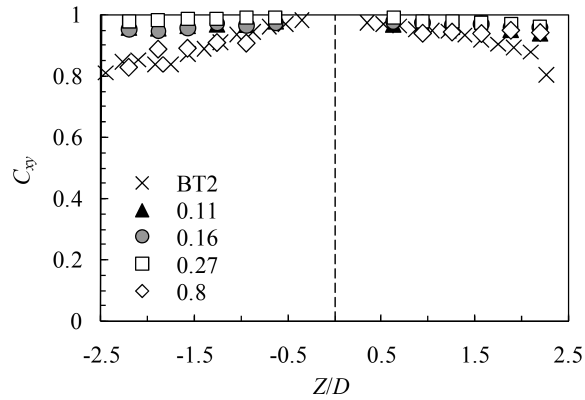

Fig. 16 Coherence distribution along the span for all finned pitches at u'_{max} point (R_e=1.1×10^5-1.9×10^5)

of coherence for s/D=0.27 were the largest in the finned tubes for all fin pitches.

CORRELATION BETWEEN SOUND AND FLOW FIELD

We measured the correlation between the aerodynamic sound and the velocity fluctuations around the finned tube to clarify the mechanism of change of the peak levels of SPL for all fin pitches. Figures 17(a)–(c) show the typical coherence at several points around a finned tube of s/D=0.16. The hot-wire sensor was set at points A, B, and C around the finned tube, as shown in Fig. 8(c). Point A was a location near the separated point of flow around the finned tube, point B was the near wake of the finned tube, and Point C was the u'_{max} point. The effect of the hot-wire probe on the aerodynamic sound was considered to be negligible, because the SPL spectrum was almost the same as the results with no hot-wire, as shown in Fig. 6. Figure 17(a) shows the results for point A. The value of coherence at the vortex shedding frequency was about 0.68. Similarly, Figs. 17(b) and (c) show the results for point B and point C, respectively. The coherences were about 0.63 and 0.44, respectively.

The coherences at vortex shedding frequencies for all fin pitches are shown in Fig. 18. The coherence values at point A and point B are larger than that of point C for all fin pitches. The Aeolian tone was correlated with the velocity fluctuations of the separation shear layer on the near surface and the near wake of the finned tube, rather than the velocity fluctuation in the wake at the u'_{max} point. Moreover, the coherence decreased for all fin pitches as the fin pitch decreased. In particular, the values of coherences at the u'_{max} point for s/D=0.16 and 0.11 were small, about 0.44 and 0.20, respectively. It was clear that the reductions in the peak SPLs for s/D=0.16 and 0.11 correlated with the decrease in the correlation between the Aeolian tone and the velocity fluctuation in the wake of the finned tube, even though the coherent distribution in the spanwise direction of the finned tube increased. It is considered that the correlations between the Aeolian tone and the velocity fluctuations for s/D=0.16 and 0.11 became weak because the velocity gradients were weak in the separation shear layer due to the small gaps of the serrated fins.

On the other hand, the coherence values at the u'_{max} point for s/D=0.80 and 0.27 were about 0.84 and 0.83, respectively. It is considered that the increase in the peak SPL for s/D=0.27 was caused by the increase in the coherent distribution in the spanwise direction, because the Aeolian tone correlated with the velocity fluctuation in the wake of the finned tube.

DYNAMIC LIFT AND SEPARATION SHEAR LAYER

It is known that the intensity of the Aeolian tone radiated from a circular cylinder depends on the dynamic lift force due to vortex shedding [9]. We measured the dynamic lifts by using a load cell. The lift force, F_L, acting on the finned tube changed sinusoidally. The period of the lift fluctuations was in agreement with the inverse of the vortex shedding frequency. The lift coefficient is defined as follows:

$$C_L = \frac{\widetilde{F}_L}{\left(\frac{1}{2}\rho U_\infty^2 D_e\right)} \tag{3}$$

where ρ is the fluid density and $\widetilde{F}_L$ is the r.m.s. amplitude of the dynamic lift per unit length at the vortex shedding frequency.

Figure 19 shows the lift coefficient ratios of finned tube C_L and bare tube C_{L0}. The values of C_{L0} are the results of BT2 for s/D=0.16 and 0.11 and BT1 for s/D=0.27 and 0.80, because the equivalent diameters of the finned tubes are almost the same as the diameters of these bare tubes. The Reynolds numbers for the lift force measurements for finned tubes were close to those of the bare tubes, because the load cell signals included the noises of natural frequency and its overtone. The lift coefficients for s/D=0.16 and 0.11 decreased compared with BT2, and that for s/D=0.27 increased compared with BT1. The lift coefficients for s/D=0.80 agreed with BT1. These are the same tendencies as the variation of SPL in Fig. 6.

The turbulence intensity in the near wake of the finned tube decreased as the pitch of the fins decreased, as shown in Figs. 9 and 11. The velocity fluctuations at the near wake were caused by the fluctuation of the free shear layer separated from the surface of the finned tube. Thus, the separation shear layers in the near wake for s/D=0.16 and 0.11 were stable compared with that of the bare tube. It is considered that if the separation

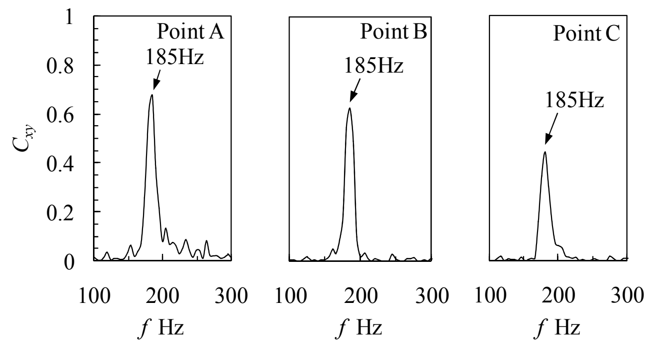

Fig. 17 Coherence between aerodynamic sound and velocity fluctuations (Point A:(0, 59), Point B:(29, 29), Point C:u'_{max} point, s/D=0.16, R_e=1.9×10^5)

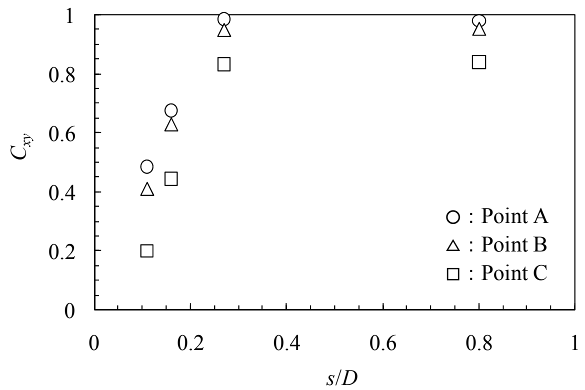

Fig. 18 Coherence between aerodynamic sound and velocity fluctuations for all fin pitches (Point A:(0, 59), Point B:(29, 29), Point C:u'_{max} point, s/D=0.16, R_e=1.1×10^5-1.9×10^5)

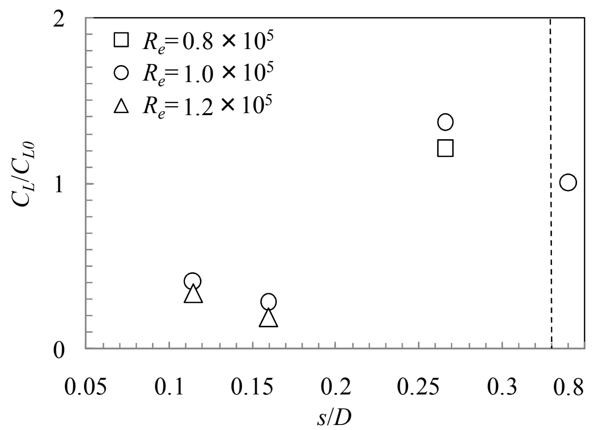

Fig. 19 Variation in dynamic lift coefficient against fin pitch ratio

shear layers in the near wake were stable, the vortex formation locations were shifted to the downstream side, the pressure fluctuation around the finned tube decreased, and finally the lift fluctuation became weak. As a result, the correlation between the sound and the velocity fluctuations in the wake of the finned tube became weak, and the Aeolian tone radiated from the finned tube decreased compared with BT2.

On the other hand, although the separation shear layers in the near wake for s/D=0.27 were somewhat stable compared with that of the bare tube, the vortex formation locations were near the finned tube, and the coherent distribution in the spanwise direction as larger than that for all fin pitches. As a result, the correlation between the sound and the velocity fluctuations in the wake of the finned tube became intense, and the Aeolian tone and lift fluctuation of the finned tube increased compared with BT1.

CONCLUSIONS

The effect of twist-serrated fins around a bare tube on the Aeolian tone was experimentally investigated and the results were compared with those of bare tubes with diameters that were the same as the tube diameter and the fin diameter. The fins were mounted spirally around a bare tube surface and had the same geometry as those actually used in boiler tubes. We measured the characteristics of the velocity fluctuation, spanwise coherence structure of the Karman vortex, dynamic lift force, and SPL of aerodynamic noise for finned tubes with various fin pitches. Furthermore, the correlation analysis between the flow field and the Aeolian tone was carried out. As a result, the following conclusions were obtained.

1. The Aeolian tone induced by Karman vortex shedding was observed in the case of a finned tube, although the complicated fin was mounted around a bare tube. The peak SPL of the spectrum varied with the fin pitch. The peak SPL for a fin pitch per tube diameter ratio of 0.27 was approximately 3 dB higher than that for a bare tube. However, for the ratios of fin pitch per tube diameter of 0.16 and 0.11, the peak SPLs were approximately 11.9 and 15.8 dB lower than those for bare tubes with the fin diameters, respectively.
2. There were two regions where the velocity fluctuation became intense, on both sides just downstream of a finned tube. As the pitch of the fins decreased, the turbulence intensity in the near wake of the finned tube decreased and the locations of the maximum turbulence intensity moved to the downstream side overall. In addition, the coherence between the Aeolian tone and the velocity fluctuation in the wake of the finned tube became weak as the fin pitch decreased. The peak SPLs decreased for small fin pitches.
3. As the Reynolds number increased, the maximum values of turbulence intensity decreased slightly for a ratio of fin pitch per tube diameter of 0.16, and its location moved to the downstream side. However, the turbulence intensities at the near wake of a finned tube were approximately the same for Reynolds numbers between 3.1×10^4 and 1.9×10^5, at about 0.20.
4. A remarkable periodic velocity fluctuation caused by the Karman vortex shedding was observed even in the wake of the finned tube. The peak frequencies of the velocity fluctuations were in good agreement with those of the SPLs. The peak frequency of the spectrum increased in proportion to the freestream velocity as the Reynolds number ranged from 1.1×10^4 to 5.5×10^4. However, for the ratios of fin pitch per tube diameter of 0.16 and 0.11, the peak frequencies were close to those of bare tubes with fin diameters at Reynolds numbers ranging from 7.6×10^4 to 1.9×10^5.
5. The equivalent diameter as the characteristic length of a finned tube for Karman vortex shedding depended on the Reynolds number. We modified the equation to calculate the characteristic diameter of the finned tube to calculate the Strouhal number. The vortex shedding frequency could be estimated by this method, as well as the bare tube, in a manner similar to the Strouhal number.
6. The spanwise scale of the Karman vortex formed in the wake of the finned tube for all fin pitches was slightly larger than that of a bare tube. This coherent scale for a ratio of fin pitch per tube diameter of 0.27 became the largest for all the fin pitches.
7. The dynamic lift coefficients for the ratios of fin pitch per tube diameter of 0.16 and 0.11 decreased compared with those for a bare tube, and that for a ratio of 0.27 increased. These tendencies were the same as the variation of the peak SPLs.

ACKNOWLEDGMENTS

The work was partially supported by the Grant-in-Aid for Scientific Research No. 20560222 from the Japan Society for Promotion of Science (in the Japan Ministry of Education and Science) for which the authors wish to express their sincere gratitude.

REFERENCES

(1) Païdoussis, M. P., A Review of Flow-induced Vibrations in Reactors and Reactor Components , Nuclear Engineering and Design, 74, (1982), pp.31–60.
(2) Pettigrew, M. J., Taylor, C. E., Vibration analysis of shell-and tube heat exchangers: an overview-Part1:flow, damping, fluidelastic instability, Journal of Fluids and Structures, 18, (2003), pp.469-483.
(3) Pettigrew, M. J., Taylor, C. E., Vibration analysis of shell-and tube heat exchangers: an overview-Part2:vibration response, fretting-wear, guidelines, Journal of Fluids and Structures, 18, (2003), pp.485-500.
(4) Ziada, S., Vorticity shedding and acoustic resonance of tube bundles, Journal of the Brazilian Society of Mechanical Sciences and Engineering, 28, (2006), pp.186-199.

(5) Owen, P. R., Buffeting excitation of boiler tube vibration, Journal of Mechanical Engineering Science, 7, (1965), pp.431–439.
(6) Chen, Y. N., Flow-induced Vibration and Noise in Tube-bank Heat Exchangers due to Von Karman Streets, Transactions of ASME, Journal of Engineering for Industry, Series B, Vol. 94, (1968), pp. 134–146.
(7) Weaver, D. S., Vortex shedding and acoustic resonance in heat exchanger tube arrays, In Technology for the 90's, ASME, (1993), pp.776–810.
(8) Ziada, S., Oengören, A., Vortex shedding in an in-line tube bundle with large tube spacings, Journal of Fluids and Structures, 7, (1993), pp.661–687.
(9) Blevins, R. D., Flow-induced vibration, R. E. Krieger Publishing Company, (1986).
(10) Zdravkovich, M. M., Review and Classification of Various Aerodynamic and Hydrodynamic Means for Suppressing Vortex Shedding, Journal of Wind Engineering and Industrial Aerodynamics, 7, (1981), pp.145-189.
(11) Nemoto, A., Yamada, M., Flow-induced Acoustic Resonance Caused by Fin-tube Bundles, ASME PVP-Vol. 243, Symposium on Flow-induced Vibration and Noise, Vol.4, (1992), pp.137-152.
(12) Nemoto, A., Yamada, M., Flow-induced Acoustic Resonance in Staggered tube banks, ASME PVP-Vol. 273, Symposium on Flow-induced Vibration and Noise, (1994), pp.273-282.
(13) Nemoto, A., Takakuwa, A., Tsutsui, M., Flow- induced Acoustic Resonance with Various Finned Tube Banks, Flow-induced Vibration and Noise, ASME, Vol.2, AD-Vol.53-2, (1997), pp.311-320.
(14) Kouba, J., Vortex Shedding and Acoustic Emission in Finned Tube Banks Exposed to Cross Flow, ASME Pressure Vessels and Piping Conference, Vol.104, (1983), pp.213-217.
(15) Hamakawa, H., Fukano, T., Nishida, E., Vortex Shedding from Serrated-Fin-Tube Banks, 6th AIAA/CEAS Aeroacoustics Conference, Paper No.2000-2001, (2000), pp.1-8.
(16) Hamakawa, H., Fukano, T., Nishida, E., Aragaki, M., Vortex Shedding from a Circular Cylinder with Fin, 7th AIAA/CEAS Aeroacoustics Conference, Paper No.2001-2215, (2001), pp.1-7.
(17) Kawaguchi, K., Okui, K., Kawabe, Y., Vortex Generation Characteristics of Serrated Finned Tube Banks with Staggered Arrangement, Turbomachinery, Vol.3, (2003), pp.181-189.
(18) Ziada, S., Jebodhsingh, D., Weaver, D. S., Eisinger, F. L., The Effect of Fins on Vortex Shedding from a Cylinder in Cross-flow, Journal of Fluids and Structures, 21, (2005), pp.689-705.
(19) Hamakawa, H., Nakashima, K., Kudo, T., Nishida, E., Fukano, T., Vortex Shedding from A Circular Cylinder with Spiral Fin, Journal of Fluid Science and Technology, Vol.3, No.6, (2008), pp.787-795.
(20) Mair, W. A., Jones, P. D. F., Palmer, R. K. W., Vortex Shedding from Finned Tubes, Journal of Sound and Vibration, Vol.39 (3), (1975), pp.293-296.
(21) Suzuki, S., Ugai, Y., Maruta, Y., Mori, S., Noise Prevention in Tube-Type Heat Exchangers Employed in Gas Turbines, Trans. Jpn. Soc. Mech. Eng., (in Japanese), Vol.52B, No.477, (1986), pp.2137-2142.
(22) Hamakawa, H., Nakashima, K., Matsue, H., Reduction of Noise Generated from Small Wind Tunnel, Proceedings of the Second Asian Joint Workshop on Thermophysics and Fluid Science, Luoyang, China, (2008), pp.12-126.
(23) Fujita, H., Shiraishi, J., Kurita, T., Maruta, Y., Yamada, S., Experimental Study on Aerodynamic Noise Generated from Two-Dimensional Models, Transactions of JSME, Vol.62, No.593B, (1996), pp.187-193.